Ambiguity Resolution in Interferometry

ERNEST JACOBS, Senior Member, IEEE
ELIZABETH W. RALSTON
Aerospace Corporation

Abstract

A comprehensive theory of interferometry from a system viewpoint with particular emphasis on the ambiguity resolution problem is developed. The derived error equations include contributions from all system uncertainties, i.e., phase measurement, frequency, and element phase center position errors in three dimensions.

The direction-of-arrival errors are inversely proportional to the interferometer baseline and it is customary to make the baseline large enough to meet the accuracy requirements. A system with a baseline greater than a half-wavelength results in the well known direction-of-arrival ambiguity problem with the addition of a third element to each baseline being a common method for resolving the ambiguity. It is shown that contrary to previous thinking there are many equally optimal positions for adding the third element to resolve the ambiguity. In addition, it is shown how the measurement made to resolve the ambiguity can also be applied to increase the accuracy of the angle-of-arrival measurement.

A central result is the derivation of expressions specifying the probability of correct resolution of ambiguities as a function of system parameters and system errors. Moreover the concept of an acceptance criterion designed to reduce processing of erroneous measurements is developed. Narrowing the criterion reduces the percentage of data accepted for processing, but increases the probability of correct ambiguity resolution. This is analogous to the relationship between the probability of detection and the probability of false alarm in radar theory.

Manuscript received October 27, 1980; revised March 25, 1981.

Authors' address: Aerospace Corporation, PO Box 92957, Los Angeles, CA 90009.

0018-9251/81/1100-0766 $00.75 ©1981 IEEE

Introduction

An interferometer is an antenna system composed of two or more elements which is used to determine the direction-of-arrival of a received signal utilizing the measured relative phase between the various elements. It has found application to various systems for many years and there is extensive literature on the subject. The references cited at the end of this paper are representative of the works reported on interferometers. We have purposely not referenced any work which is not generally available to all readers.

What is missing in the existing literature is a complete analysis of the interferometer that ties all aspects of its operation together. In addition, the treatment of the ambiguity resolution problem has been incomplete. This paper attempts to develop a comprehensive theory of interferometry from the systems viewpoint. Error equations have been derived which include contributions from all system uncertainties, i.e., phase measurement, frequency, and element phase center position errors in three dimensions. The ambiguity resolution problem has been analyzed in detail and definitive results are presented. To the best of our knowledge, this work represents the first time that the probabilities associated with ambiguity resolution are treated.

It has been found that for any system whose baseline is large enough to have ambiguities it is not possible to resolve the ambiguities correctly 100 percent of the time. The concept of an acceptance criterion, designed to reduce the percentage of data whose ambiguities will be incorrectly resolved, is introduced. Narrowing the criterion reduces the percentage of data accepted for processing, but increases the probability of correct ambiguity resolution.

It is shown that if the interferometer is designed to resolve ambiguities at the highest frequency of operation, it will resolve ambiguities at any lower frequency with no more difficulty. Also, the number of possible modulo number combinations is less than the total number of combinations for the individual baselines. This fact reduces the required processing and has a favorable impact on the probability of resolving the ambiguity correctly.

Basic Five Element Interferometer

A basic five element interferometer is shown in Fig. 1. Elements 1, 2, 3, and 4, referred to as primary elements, are utilized to measure the direction of arrival of the incoming signal. In the initial portion of the analysis element 5 is not utilized. Subsequently it is shown that for large separation between the primary elements (which improves direction of arrival measurement accuracy), an additional element (number 5) is needed to resolve ambiguities.

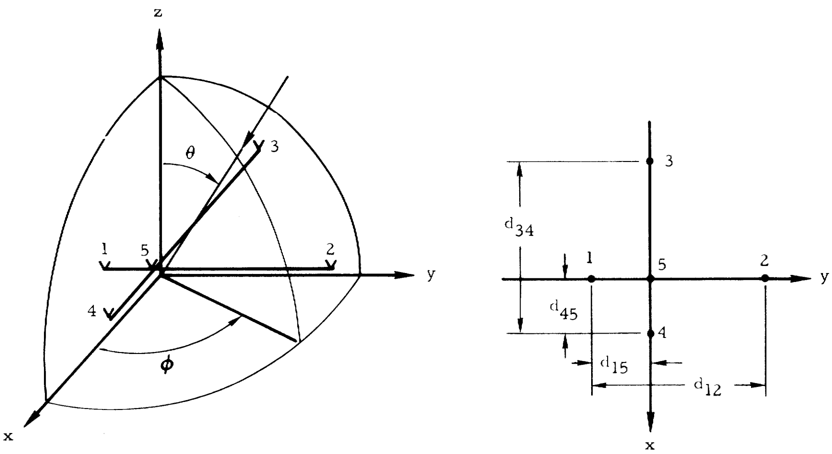

Fig. 1. Basic 5-element interferometer.

The direction of the incoming signal is determined by measuring the phase differences between the primary elements. These phase differences are related to the other system parameters as follows:

$$\psi_{12} = (2\pi d_{12}/\lambda)\sin\theta\sin\phi \tag{1a}$$

$$\psi_{34} = (2\pi d_{34}/\lambda)\sin\theta\cos\phi \tag{1b}$$

where ψ_{ij} is the phase by which element i lags j (radians), λ is the wavelength of the radiated frequency f, d_{ij} is the separation of elements i and j, and θ, ϕ are the spherical coordinates specifying the direction of arrival of the signal. It is assumed $0 \leqslant \theta \leqslant \pi/2$, i.e., the signal is coming from the upper hemisphere.

If ψ_{12} and ψ_{34} are known, the direction of arrival of the incoming signal can be computed from the following expressions:

$$\theta = \sin^{-1}[(\psi_{12}\lambda/2\pi d_{12})^2 + (\psi_{34}\lambda/2\pi d_{34})^2] \tag{2}$$

$$\phi = \tan^{-1}[(\psi_{12}\, d_{34}/\psi_{34}\, d_{12})] \tag{3}$$

where the angle defined by ϕ lies in the same quadrant as (ψ_{34}, ψ_{12}).

Equations (1a) and (1b) are based on the assumption that the phase centers of all the antennas are in a plane and that the two baselines are orthogonal. This is the nominal configuration. However, to derive estimates of the error statistics for the direction of arrival, one must use more general expressions in which deviations from the norm can be accounted for. The more general formulas are

$$\psi_{12} = (2\pi/\lambda)\,\bar{p}_{12}\cdot\bar{r} = (2\pi/\lambda)[(x_2 - x_1)\sin\theta\cos\phi + (y_2 - y_1)\sin\theta\sin\phi + (z_2 - z_1)\cos\theta] \tag{4a}$$

$$\psi_{34} = (2\pi/\lambda)\,\bar{p}_{34}\cdot\bar{r} = (2\pi/\lambda)[(x_4 - x_3)\sin\theta\cos\phi + (y_4 - y_3)\sin\theta\sin\phi + (z_4 - z_3)\cos\theta] \tag{4b}$$

where $\bar{p}_{ij}$ is the vector connecting elements i and j, $\bar{r}$ is the unit vector in the direction of arrival, and x_i, y_i, and z_i are the positions of antenna element i. In the nominal (zero-error) case, $x_1 = x_2 = y_3 = y_4 = z_1 = z_2 = z_3 = z_4 = 0$.

For small errors in the direction of arrival, the error can be approximated by linearization of (4a) and (4b). This approximation is made assuming that the separations between phase centers are much larger than their uncertainties, that the system parameter errors have Gaussian distributions with zero means, and that the errors in the system parameters are statistically independent.

The error statistics for the direction of arrival can be specified by giving the entries in the covariance matrix for (θ, ϕ); errors in θ and ϕ are in orthogonal directions, but an error in ϕ corresponds to a smaller direction-of-arrival error than an equal error in θ by a factor of *sin* θ. Scaling by this factor, one can express the error statistics in a plane perpendicular to the direction of arrival. Letting U and V measure direction-of-arrival error in the directions of change of θ and ϕ, the elements of the covariance matrix for (U, V) are given by

$$\sigma^2(U) = \sigma^2(\theta) \approx \sum (\partial\theta/\partial\varrho_i)^2\,\sigma^2(\varrho_i) \tag{5}$$

$$\sigma^2(V) = \sin^2\theta\,\sigma^2(\phi) \approx \sin^2\theta \sum (\partial\phi/\partial\varrho_i)^2\,\sigma^2(\varrho_i) \tag{6}$$

$$\sigma(U, V) = \sin\theta\,\sigma(\theta, \phi) \approx \sin\theta \sum (\partial\theta/\partial\varrho_i)\cdot(\partial\phi/\partial\varrho_i)\,\sigma^2(\varrho_i). \tag{7}$$

where the ϱ_i are the system parameters subject to error.

The partial derivatives in (5), (6), and (7) can be obtained from (4a) and (4b). The expressions for $\sigma^2(U)$, $\sigma^2(V)$, and $\sigma(U, V)$ are complex and can be greatly simplified when the symmetry which exists in most practical systems is introduced. This symmetry is as follows:

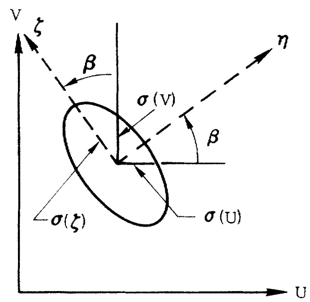

Fig. 2. Error ellipse.

1) The baselines of both arms of the interferometer are the same, i.e.,

$$d_{12} = d_{34} = d.$$

2) The variances of the phase measurements in both arms are the same, i.e.,

$$\sigma^2(\psi_{12}) = \sigma^2(\psi_{34}) = \sigma^2(\psi).$$

3) The variances of the baseline errors are the same, i.e.,

$$\sigma^2(y_1) = \sigma^2(y_2) = \sigma^2(x_3) = \sigma^2(x_4) = \sigma^2(d/2).$$

Notice that $\sigma^2(d/2)$ is the variance of each arm.

4) The variances of the tilt errors out of the plane of the interferometer are the same for both arms, i.e.,

$$\sigma^2(z_1) = \sigma^2(z_2) = \sigma^2(z_3) = \sigma^2(z_4) = \sigma^2(z).$$

5) The variances of the tilt errors in the plane of the interferometer are the same for both arms, i.e.,

$$\sigma^2(x_1) = \sigma^2(x_2) = \sigma^2(y_3) = \sigma^2(y_4) = \sigma^2(N).$$

Using the above symmetry, the covariance matrix for (U, V) has entries:

$$\sigma^2(U) \approx [\lambda\sigma(\psi)/2\pi d \cos\theta]^2 + [\tan\theta\, \sigma(f)/f]^2 + 2[\sigma(z)/d]^2 + [\tan^2\theta(1 + \cos^2 2\phi)/d^2] \cdot \sigma^2(d/2) + [\tan\theta \sin 2\phi\, \sigma(N)/d]^2 \tag{8}$$

$$\sigma^2(V) \approx [\lambda\sigma(\psi)/2\pi d]^2 + 2[\cos\theta\sigma(z)/d]^2 + [\sin\theta \sin 2\phi\sigma(d/2)/d]^2 + [\sin^2\theta(1 + \cos^2 2\phi)/d^2]\,\sigma^2(N) \tag{9}$$

$$\sigma(U, V) \approx (\sin\theta \tan\theta \sin 4\phi/2d^2)[\sigma^2(N) - \sigma^2(d/2)]. \tag{10}$$

The more general expressions are given in the appendix.

For systems where the phase measurement error component dominates, the above expressions reduce to

$$\sigma^2(U) \approx [\lambda\sigma(\psi)/2\pi d \cos\theta]^2 \tag{11}$$

$$\sigma^2(V) \approx [\lambda\sigma(\psi)/2\pi d]^2 \tag{12}$$

$$\sigma(U, V) \approx 0. \tag{13}$$

Equation (11) is sometimes quoted as the error equation for an interferometer.

The covariance matrix for (U, V) determines an error ellipse in a plane normal to the direction of arrival. This ellipse is not necessarily oriented along a coordinate axis (Fig. 2). The orientation of the ellipse relative to (U, V) axis is given by the angle β where [17]

$$\tan 2\beta = 2\sigma(U, V)/[\sigma^2(U) - \sigma^2(V)]. \tag{14}$$

The axes of the new coordinate system correspond to the ellipse axes and the new variables η and ζ in this coordinate system have variances given by

$$\sigma^2(\eta) = \sigma^2(U)\cos^2\beta + \sigma(U, V)\sin 2\beta + \sigma^2(V)\sin^2\beta \tag{15}$$

$$\sigma^2(\xi) = \sigma^2(V)\cos^2\beta + \sigma(U, V)\sin 2\beta + \sigma^2(U)\sin^2\beta. \tag{16}$$

The (η, ξ) axes represent the directions of maximum and minimum angular errors.

The error expressions (8), (9), and (10) are for the direction of arrival measured with respect to the boresight of the interferometer reference coordinate system. If there is an uncertainty in the position of the boresight of the reference plane, the covariance matrix for the boresight coordinates must be added to the previously computed covariance matrix to give the overall direction-of-arrival error statistics. If the covariance between U and V is zero, this just corresponds to forming the rms of the two sets of errors.

Examination of the error equations shows that the baseline length has considerable effect on the amount of error. A convenient way to reduce the direction-of-arrival error is to make the baseline as large as possible without disturbing its error statistics appreciably.

Ambiguity Resolution Using Auxiliary Restricted Short Baseline

Whenever the baseline of the interferometer is > $\lambda/2$, the possible range of phase differences can exceed 2π. For example, for a 10λ baseline, the phase differences for the entire upper hemisphere can vary between -20π and $+20\pi$. Unfortunately the measurement of phase difference can almost always only be made modulo 2 π. For instance, if the actual phase difference is 16.25π, measurement would indicate a difference of 0.25π. This leads to an ambiguity in determining the direction of the incoming signal.

The purpose of adding the fifth element is to resolve the ambiguity. By selecting the proper spacings, the addition of the one element (number 5) can resolve the ambiguities in both planes. An obvious solution for resolving the ambiguities is to make the separations d_{15} and d_{45} less than a half-wavelength for the highest operational frequency. The phase differences (ψ_{15}, ψ_{45}), are measured using the short baselines and from these measurements an estimate is made of what the phase measurements should be for the long baselines. If the estimate of the phase difference is close to one of the possible solutions of the phase difference for the long baseline, the ambiguity will be resolved. Subsequently, it is shown what is meant by close with an expression for determining the probability of resolving the ambiguity as a function of the uncertainties in the phase estimate and phase measurement.

The phase estimates for the long baselines, ψ_{12e} and ψ_{34e}, are given by

$$\psi_{12e} = (d_{12}/d_{15})\,\psi_{15} \tag{17a}$$

$$\psi_{34e} = (d_{34}/d_{45})\,\psi_{45}. \tag{17b}$$

The convention here and throughout this paper is that the measured phase differences lie between $-\pi$ and $+\pi$.

By taking the total derivative of (17), expressions for the errors in phase estimates can be approximated. Assuming that the phase center separation errors and phase difference measurement errors are statistically independent and have zero means, the following approximations for the variances of the phase estimate errors are derived:

$$\sigma^2(\psi_{12e}) \approx [(d_{12}/d_{15})\,\psi_{15}]^2\,[(\sigma(d_{12})/d_{12})^2 + (\sigma(d_{15})/d_{15})^2 + (\sigma(\psi_{15})/\psi_{15})^2] \tag{18a}$$

$$\sigma^2(\psi_{34e}) \approx [(d_{34}/d_{45})\,\psi_{45}]^2\,[(\sigma(d_{34})/d_{34})^2 + (\sigma(d_{45})/d_{45})^2 + (\sigma(\psi_{45})/\psi_{45})^2]. \tag{18b}$$

For systems where the phase measurement error component dominates, the phase estimate error approximation can be reduced to the following:

$$\sigma(\psi_{12e}) \approx (d_{12}/d_{15})\,\sigma(\psi_{15}) \tag{19a}$$

$$\sigma(\psi_{34e}) \approx (d_{34}/d_{45})\,\sigma(\psi_{45}). \tag{19b}$$

Probability of Resolving Ambiguities Utilizing Phase Estimate

It is assumed that the system consists of a long baseline interferometer which is utilized to make the direction-of-arrival measurement. However, since this baseline is more than $\lambda/2$, the possible phase differences will exceed 2π and there will be ambiguities. By some other means (e.g., an interferometer with element spacing of $\lambda/2$) an estimate is made of what the phase measurement of the long baseline interferometer should be. This estimate will then be used to resolve the ambiguity of the long baseline interferometer. This section develops general expressions for the probability the data will be accepted for processing and the probability that the ambiguity is resolved correctly on condition that it is accepted for processing as a function of the acceptance criterion and the error statistics of the phase measurement and estimate.

The development is for only one arm of the interferometer system. The expressions for the other arm are exactly the same. The probability for the interferometer system is the product of the probabilities for the individual arms.

Let ψ_{12} be the phase difference for the long baseline interferometer and ψ_e be the estimate of ψ_{12} based on the short baseline measurement. The phase difference for the long baseline interferometer can only be measured modulo 2π; let ψ_d be the modulo 2π measurement and $\overline{\psi}_d$ the mean of its distribution. The standard deviations for ψ_d and ψ_e are $\sigma(\psi_d)$ and $\sigma(\psi_e)$. The situation is as shown on Fig. 3. The centers of the possible solutions for the long baseline interferometer are shown below the axis and are labeled $\ldots, \overline{\psi}_d - 6\pi, \overline{\psi}_d - 4\pi, \overline{\psi}_d - 2\pi, \overline{\psi}_d, \overline{\psi}_d + 2\pi, \overline{\psi}_d + 4\pi, \overline{\psi}_d + 6\pi, \ldots$.

The estimate of the phase difference ψ_e and the mean of its distribution $\overline{\psi}_e$ are shown above the axis. The estimate is used to select $\psi_d + \hat{n}\,2\pi$, where $\hat{n}$ is determined as the correct modulo number and thus resolves the ambiguity. It is assumed that the biases have been removed from the system and the mean of the estimate distribution is equal to the mean of the correctly resolved distribution, i.e., $\overline{\psi}_e = \overline{\psi}_d + \hat{n}\,2\pi$ (in Fig. 3, $\overline{\psi}_e = \overline{\psi}_d + 2\pi$).

Let us define $D(n)$, the difference between the phase estimate and the possible solutions of the long baseline interferometer, as follows:

$$D(n) = |\psi_e - (\psi_d + n2\pi)| \tag{20}$$

where n is an integer limited by

$$|n| \leqslant (d_{12}/\lambda)\sin\theta_{\max} + \tfrac{1}{2} \tag{21}$$

In many instances it is desired that the interferometer system only operate over a region which is less than a full hemisphere. As can be seen from

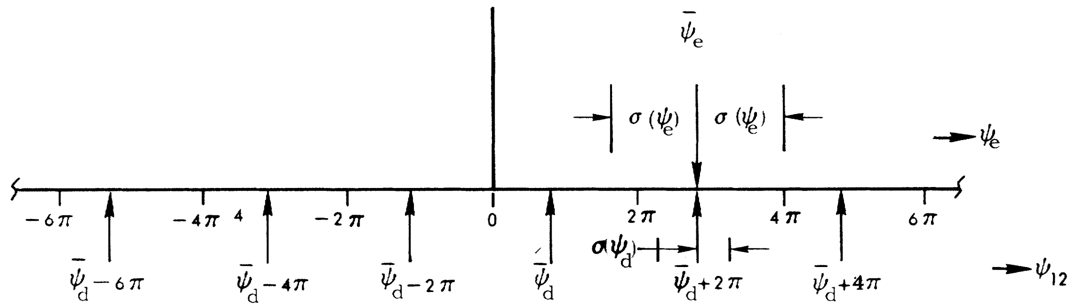

Fig. 3. Phase plot.

(21), this will make the ambiguity resolution problem less difficult because there are fewer valid modulo numbers and the possible number of solutions is less.

The coverage region reduction also increases the maximum allowable spacing the short baseline interferometer can have without being subject to ambiguous solutions. Instead of $\lambda/2$, the restriction is

$$d_{15} < (\lambda/2)(1/\sin\theta_{max}). \tag{22}$$

Notice that the limit θ_{max} is more than just a boundary beyond which the data is not needed. To avoid making erroneous measurements, the system must either not have the capability of receiving signals originating outside the θ_{max} boundary or must suppress such signals.

All possible values of n are substituted into (20) and a modulo number N is found such that $D(N) = D_{min}$. The decision is made to reduce the data when

$$D_{min} \leqslant k_a \pi \tag{23}$$

where k_a is the criterion selected for accepting data and is restricted to $0 < k_a \leqslant 1$. For the selected k_a, $\sigma(\psi_e)$, and $\sigma(\psi_d)$, expressions are developed for P_r, the probability that the data will be reduced, and P_c, the probability that the ambiguity will be resolved correctly on the condition it has been accepted for reduction.

The probability that the data will be reduced is given by

$$P_r = \sum_n P[-k_a\pi < \psi_e - (\psi_d + n\,2\pi) < k_a\pi]. \tag{24}$$

Rewriting (24) it becomes

$$P_r = \sum_n P[-k_a\pi + (n-N)2\pi < \psi_e - (\psi_d + N2\pi) < k_a\pi + (n-N)2\pi] \tag{25}$$

where N is the correct modulo number.

Let $n = N + k$, where $k = 0, \pm 1, \pm 2, \ldots$. Substituting this change of variables in (25) will center the expansion around the true modulo number.

$$P_r = \sum_k P[-k_a\pi + k\,2\pi < \psi_e - (\psi_d + N2\pi) < k_a\pi + k\,2\pi]. \tag{26}$$

Assuming the error functions of ψ_e and ψ_d are Gaussian with zero means and are statistically independent, (24) can be expanded as follows:

$$P_r = \sum_k \operatorname{erf}[(k_a + 2k)\pi/\sqrt{2[\sigma^2(\psi_e) + \sigma^2(\psi_d)]}\,] \tag{27}$$

where $k = 0, \pm 1, \pm 2, \ldots$, and $\operatorname{erf}(x) = (2/\sqrt{2}) \times \int_0^x e^{-t^2}dt$.

To determine the required number of terms for (27), let $k_a = 1$ and keep adding terms until $P_r = 1$ to within the analysis precision.

The terms shown in the expansion (27) are for the case where the true modulo number N is not at an extreme. When N is at an extreme, the terms of (27) other than the term with $k = 0$ are multiplied by $\frac{1}{2}$. This "edge effect" is ignored for the computed probability curves.

The probability that the ambiguity is resolved correctly on condition it has been accepted for reduction is

$$P_c = P[k = 0 \mid -k_a\pi < \psi_e - [\psi_d + 2\pi(N+k)] < k_a\pi]$$

$$P_c = \operatorname{erf}[k_a\pi/\sqrt{2[\sigma^2(\psi_e) + \sigma^2(\psi_d)]}\,]/P_r. \tag{28}$$

Plots of P_r and P_c as a function of the selection criterion k_a are given in Figs. 4 through 8 for phase measurement error standard deviations of 1 to 5 electrical degrees. These plots are parameterized for various values of phase estimation error standard deviations. In general the phase measurement error statistics are the same for both the short and long baseline interferometers. However the error in the phase estimate of the long baseline interferometer is proportional to the ratio of the baselines for systems where the phase measurement error dominates (19a and 19b). For this reason the phase estimate standard deviations are much higher.

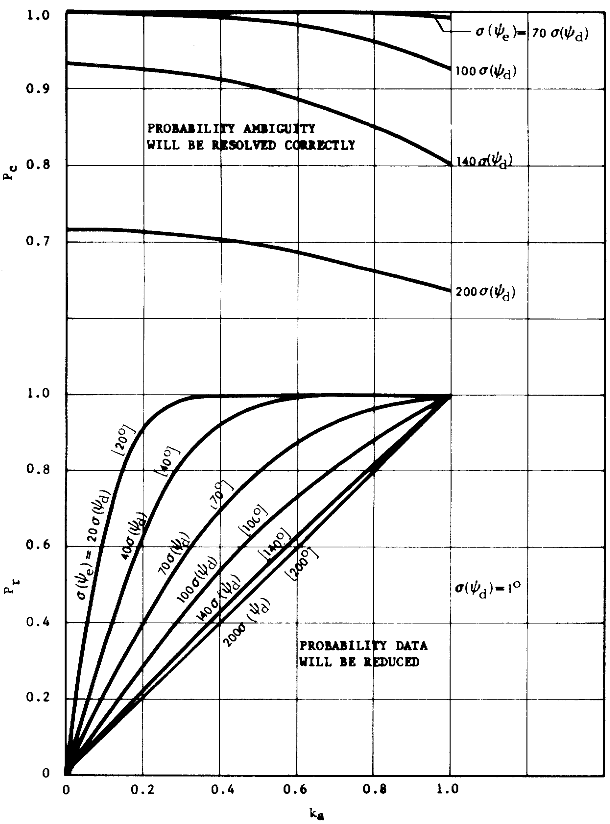

Fig. 4. Interferometer probability curves for 1° (1σ) phase measurement error.

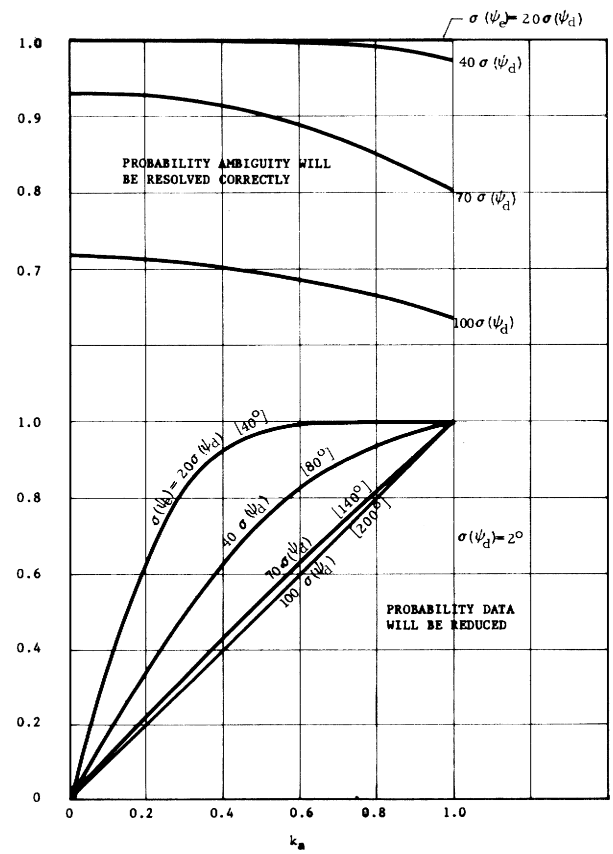

Fig. 5. Interferometer probability curves for 2° (1σ) phase measurement error.

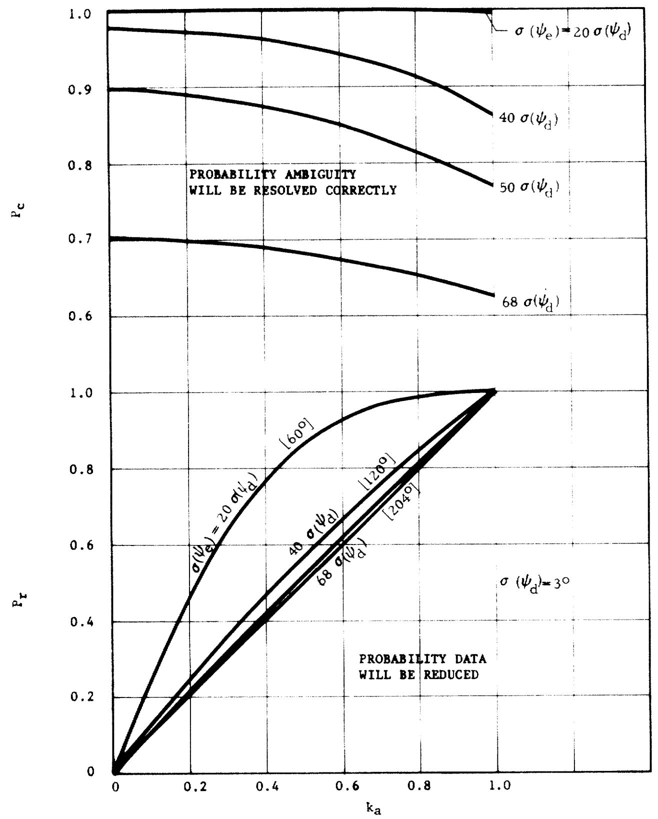

Fig. 6. Interferometer probability curves for 3° (1σ) phase measurement error.

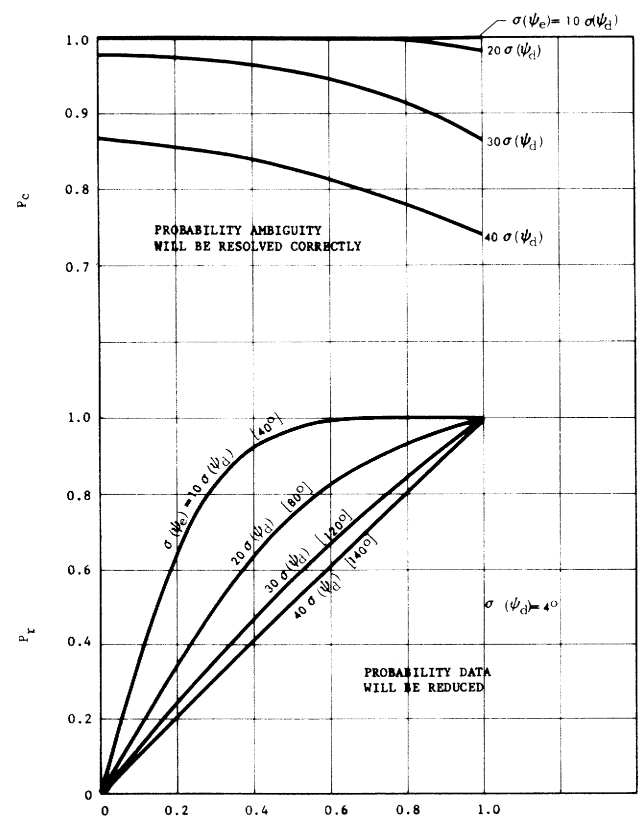

Fig. 7. Interferometer probability curves for 4° (1σ) phase measurement error.

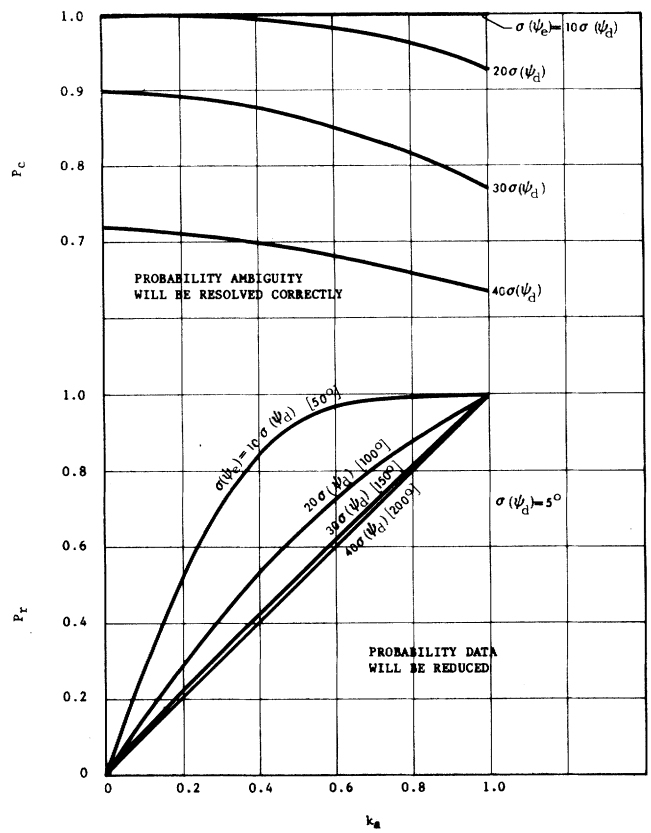

Fig. 8. Interferometer probability curves for 5° (1σ) phase measurement error.

Notice that the probabilities are for one arm of the interferometer. The probability for a system is the product of the probabilities of the individual arms.

Optimal Design for Auxiliary Unrestricted Short Baseline

Unfortunately it is sometimes not physically possible to obtain separations as small as $\lambda/2$ at the highest frequency of operation. This section treats the problem of ambiguity resolution when the short baseline can have length greater than $\lambda/2$.

In this derivation it is assumed that the highest frequency is used (shortest wavelength). It will be shown subsequently that if the configuration resolves the ambiguities at the highest frequency, it is no more difficult to resolve the ambiguities at any lower frequency.

Since measurements of phase difference can only be made modulo 2π,

$$\psi_{12} = \psi_{12}^{*} + n_{12}2\pi \tag{29a}$$

$$\psi_{15} = \psi_{15}^{*} + n_{15}2\pi \tag{29b}$$

where ψ_{12}^{*} and ψ_{15}^{*} are the phase differences modulo 2π, chosen to be between $-\pi$ and $+\pi$. The symbols n_{12} and n_{15} are integers limited by

$$|n_{12}| \leqslant (d_{12}/\lambda)\sin\theta_{\max} + \tfrac{1}{2} \tag{30a}$$

$$|n_{15}| \leqslant (d_{15}/\lambda)\sin\theta_{\max} + \tfrac{1}{2}. \tag{30b}$$

It is assumed that the interferometer only operates in the upper hemisphere and thus $\theta_{\max} \leqslant \pi/2$.

Substituting (29) into (1) one obtains

$$\psi'_{12} + n_{12} = (d_{12}/\lambda)u \tag{31a}$$

$$\psi'_{15} + n_{15} = (d_{15}/\lambda)u \tag{31b}$$

where ψ'_{12} and ψ'_{15} are ψ_{12}^{*} and ψ_{15}^{*} normalized by 2π (referred to as phase in units of turns) and vary between $-1/2$ and $+1/2$; $u = \sin\theta\sin\phi$.[1]

Combining (31a) and (31b) by eliminating u, one obtains

[1]Notice that for the other arm of the interferometer $u = \sin\theta \times \cos\phi$.

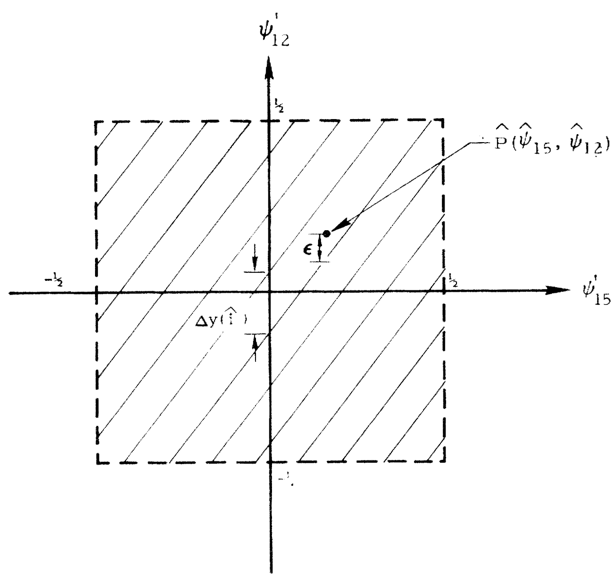

Fig. 9. Phase sample space.

$$\psi'_{12} = (d_{12}/d_{15})\,\psi'_{15} + (d_{12}/d_{15})\,n_{15} - n_{12}. \tag{32}$$

Rewriting (32) it becomes

$$d_{12}\,n_{15} - d_{15}\,n_{12} = d_{15}\,\psi'_{12} - d_{12}\,\psi'_{15}. \tag{33}$$

Since ψ_{12}' and ψ_{15}' vary between $-1/2$ and $+1/2$, (32) is further restricted to valid valid pairs of modulo numbers by

$$|d_{15}n_{12} - d_{12}n_{15}| \leqslant \tfrac{1}{2}\,(d_{12} + d_{15}). \tag{34}$$

For any choice of n_{12} and n_{15}, (32) determines a line in phase space. Each line represents the relationship between ψ_{12}' and ψ_{15}' for a pair of constant n_{12} and n_{15}. Since the lines in this family have equal slopes, they are parallel. The situation is illustrated graphically in Fig. 9, where the ψ' values are restricted to the allowable range, i.e., $|\psi'| \leqslant \frac{1}{2}$.

Now suppose $\hat{\psi}_{12}$ and $\hat{\psi}_{15}$ are measured values for ψ'_{12} and ψ'_{15}. These measurements can be represented by a point $\hat{P}(\hat{\psi}_{15}, \hat{\psi}_{12})$ in the sample space. In the absence of measurement error, this point $\hat{P}$ would lie on one of the lines determined by (32). Knowing this line would determine modulo numbers n_{12} and n_{15}, which would resolve the ambiguity in the direction of arrival.

In the presence of measurement error, $\hat{P}$ will, in general, not lie on any of the lines. In this case one can determine the line closest to $\hat{P}$. This line corresponds to modulo numbers $\hat{N}_{12}$ and $\hat{N}_{15}$, which are the best estimates of the true modulo numbers.

To obtain the best estimates of the normalized phase differences, one wishes to find $\overline{\psi}_{12}$, $\overline{\psi}_{15}$ to minimize

$$D = (\overline{\psi}_{12} - \hat{\psi}_{12})^2 + (\overline{\psi}_{15} - \hat{\psi}_{15})^2 \tag{35}$$

where $\overline{\psi}_{12}$ and $\overline{\psi}_{15}$ are related by (32). The point $\overline{P}(\overline{\psi}_{15}, \overline{\psi}_{12})$ is the closest point on the line nearest to the measured point $\hat{P}(\hat{\psi}_{15}, \hat{\psi}_{12})$.

Substituting (32) into (35) one obtains

$$D = (\overline{\psi}_{12} - \hat{\psi}_{12})^2 + [(d_{15}/d_{12})\,\overline{\psi}_{12} + (d_{15}/d_{12})\,\hat{N}_{12} - \hat{\psi}_{15} - \hat{N}_{15}]^2. \tag{36}$$

The relationship to minimize D is found by setting $\partial D/\partial\,\overline{\psi}_{12}$ to zero; the minimum value of D occurs when

$$\overline{\psi}_{12} + \hat{N}_{12} = (d_{12}d_{15}/(d_{12}^2 + d_{15}^2))(\hat{\psi}_{15} + \hat{N}_{15}) + (d_{12}^2/(d_{12}^2 + d_{15}^2))(\hat{\psi}_{12} + \hat{N}_{12}). \tag{37}$$

The quantity $\overline{\psi}_{12} + \hat{N}_{12}$ computed from (37) is then the best estimate of the phase difference corresponding to the long baseline interferometer. The variance of the best estimate $\overline{\psi}_{12}$ is approximated by

$$\sigma^2(\overline{\psi}_{12}) \approx d_{12}^2\sigma^2(\psi)/(d_{12}^2 + d_{15}^2). \tag{38}$$

Equation (38) assumes the phase difference measurements $\hat{\psi}_{12}$ and $\hat{\psi}_{15}$ are independent and have the same error statistics with the mean of the measurement error equal to zero. It is interesting to notice that the best estimate of the phase difference utilizes both phase measurements. Therefore the measurement that is made primarily to resolve the ambiguity also serves to improve the accuracy of the long baseline interferometer.

A key question is to determine the probability that this procedure results in the correct resolution of ambiguity; i.e., to determine the probability that the modulo numbers chosen by this method are the correct ones. The probability formulas are developed in the following section. However the resolution of ambiguity is clearly facilitated by optimal placement of the fifth antenna. It will be shown that the optimum condition for resolving the ambiguity is that the family of lines in (32) be as widely spaced as possible, subject to whatever physical constraints exist on d_{12}/λ and d_{15}/λ.

Given d_{12}/λ, a possible choice for d_{15}/λ can be evaluated as follows. The possibilities for modulo numbers n_{12} and n_{15} are determined by (30) and (34). The line corresponding to n_{12} and n_{15} has y intercept

$$y = (d_{12}/d_{15})n_{15} - n_{12}. \tag{39}$$

The set of lines can be ordered in increasing y intercepts $y(i)$. Then the distance between adjacent y intercepts is

$$\Delta y(i) = y(i) - y(i - 1). \tag{40}$$

Fig. 10. Separation of phase lines as function of baseline.

Fig. 11. Separation of phase lines as function of baseline.

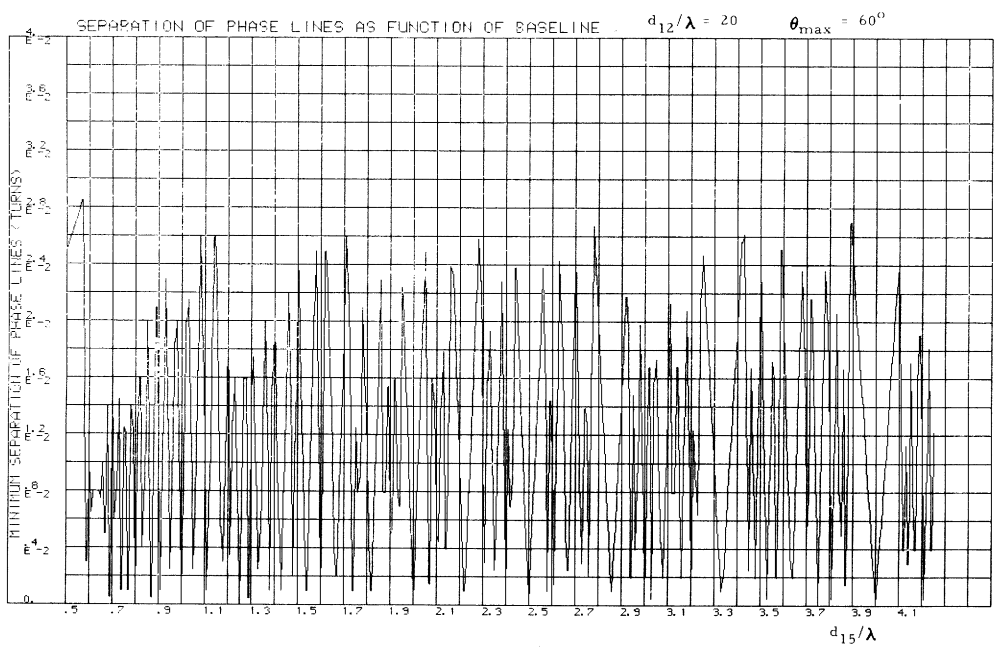

Since these lines have the same slope, which is known from (32), the separation between lines $\Delta l\,(i)$ is given by

$$\Delta\, l(i) = [y(i) - y(i-1)][1 + (d_{12}/d_{15})^2]^{-1/2}. \tag{41}$$

From this one can find the minimum separation between lines.

This evaluation procedure was programmed on a digital computer. For input values of d_{12}/λ and d_{15}/λ and θ_{max}, the program determines the distribution of the distances Δl between adjacent lines in phase space. Using this program two cases were investigated: $d_{12}/\lambda = 10$, and $d_{12}/\lambda = 20$. In each case θ_{max} was set to 60° and d_{15}/λ was varied from 0.5 to 4.9 in steps of 0.01. Figs. 10 and 11 are plots of Δl_{min} as a function of d_{15}/λ. Clearly there are several peaks in the minimum separation and each of these peaks is a possible candidate for the d_{15}/λ separation.

In the case $d_{12}/\lambda = 10$, one of the peaks is at $d_{15}/\lambda = 2.78$; as an example this separation is selected for further investigation. A tabulation of the parameters associated with this separation is given in Table I and the statistics for these parameters in Table II.

Up to this point it has been assumed that the interferometer design is one which is optimized at the

TABLE I.
Sample Space Parameter For $d_{12}/\lambda = 10$, $d_{15}/\lambda = 2.78$

y	$\Delta y(i)$	$\Delta l(i)$	n_{12}	n_{15}	$d_{15/\lambda}$
−2.194	0.000	0.000	−5	−2	2.780
−2.000	0.194	0.052	2	0	2.780
−1.806	0.194	0.052	9	2	2.780
−1.597	0.209	0.056	−2	−1	2.780
−1.403	0.194	0.052	5	1	2.780
−1.194	0.209	0.056	−6	−2	2.780
−1.000	0.194	0.052	1	0	2.780
−0.806	0.194	0.052	8	2	2.780
−0.597	0.209	0.056	−3	−1	2.780
−0.403	0.194	0.052	4	1	2.780
−0.194	0.209	0.056	−7	−2	2.780
0.000	0.194	0.052	0	0	2.780
0.194	0.194	0.052	7	2	2.780
0.403	0.209	0.056	−4	−1	2.780
0.597	0.194	0.052	3	1	2.780
0.806	0.209	0.056	−8	−2	2.780
1.000	0.194	0.052	−1	0	2.780
1.194	0.194	0.052	6	2	2.780
1.403	0.209	0.056	−5	−1	2.780
1.597	0.194	0.052	2	1	2.780

TABLE II.
Sample Space Statistics For $d_{12}/\lambda = 10$, $d_{15}/\lambda = 2.78$

Δy	Δl	Number of Cases	Fraction of Cases
0.194	0.052	14	0.6364
0.209	0.056	8	0.3636

highest frequency (shortest wavelength) of operation. The basic equations for determining the separation between lines in phase space are (39), (40), (30), and (34). Equation (30) is the only expression which is frequency dependent. This expression shows that when the frequency is less than its highest value, the only change possible is a reduction in the number of valid modulo integers. Any such reduction will reduce the number of lines in the sample space. Thus when d_{15} is selected for resolving ambiguities at the highest frequency, the difficulty in resolving the ambiguities at any lower frequency will be no greater than the difficulty at the highest frequency.

Probability Expressions

In the previous section a method for designing an interferometer to optimize ambiguity resolution was presented. In this section a criterion for accepting measurements for data reduction is developed and the probability expressions associated with the system measurement accuracies and this criterion are derived. Again, the development is for a single arm of the interferometer.

Consider an interferometer with a long baseline length of d_{12}/λ and a short baseline length d_{15}/λ. Suppose $\hat{\psi}_{12}$ and $\hat{\psi}_{15}$ are the measured values (modulo 2π) of the phase differences in turns. In the previous section it was shown that the true modulo numbers can be estimated by finding the line of (32) closest to $\hat{P}(\hat{\psi}_{15}, \hat{\psi}_{12})$. Computationally this may be done by finding the vertical distance from $\hat{P}(\hat{\psi}_{15}, \hat{\psi}_{12})$ to each line.

This distance is

$$\varepsilon = \hat{\psi}_{12} - (d_{12}/d_{15})\hat{\psi}_{15} + n_{12} - (d_{12}/d_{15})n_{15}. \tag{42}$$

By substituting all possible valid combinations of n_{12} and n_{15} into (42) the pair ($\hat{N}_{15}$, $\hat{N}_{12}$) is found which minimizes $|\varepsilon|$. The best estimate of the modulo number of the long baseline interferometer is $\hat{N}_{12}$ and the ambiguity is correctly resolved if $\hat{N}_{12} = N_{12}$, the correct modulo number.

The likelihood that this method results in correct resolution of the ambiguity is greater if the measurement pair $(\hat{\psi}_{15}, \hat{\psi}_{12})$ lies close to one of the lines in (32). Thus one can utilize an acceptance criterion under which a pair of measurements is accepted for processing only if $|\varepsilon_{\min}|$ is less than a specified fraction of the separation between lines. This criterion can be formulated as

$$|\varepsilon_{\min}| < k_b\, \Delta y\, (\hat{i}) \tag{43}$$

where $\Delta y(\hat{i})$ is the ordinate separation between the two lines which "enclose" the measurement (Fig. 9), and k_b is the acceptance criterion $(0 < k_b \leqslant \frac{1}{2})$.

The probability that a measurement is accepted for reduction is then given by

$$\begin{aligned} P_r = \sum_{\hat{N}_{12},\hat{N}_{15}} & P[- k_b\, \Delta y(\hat{i}^-) < \hat{\psi}_{12} \\ & - (d_{12}/d_{15})\, \hat{\psi}_{15} + \hat{N}_{12} - (d_{12}/d_{15})\, \hat{N}_{15} \\ & < k_b\, \Delta y(i^+)]. \end{aligned} \tag{44}$$

The distances between y intercepts are not necessarily the same and this fact is accounted for in (44). The y intercept difference between the line defined by $\hat{N}_{15}$, $\hat{N}_{12}$ and the adjacent line below it is $\Delta y(i^-)$. Similarly $\Delta y(i^+)$ is the intercept difference for the adjacent line above.

The largest contribution to this sum is the term with N_{12}, N_{15}, the true modulo numbers. Thus it is desirable to rewrite this sum so that it is centered about this pair, in order that the sum can be approximated with adequate accuracy using a minimum number of terms.

To rewrite (44) let the lines in (32) be ordered in increasing y intercepts. All operations will be centered around the correct y intercept, i.e., $y(0) = (d_{12}/d_{15})N_{15} - N_{12}$. The increments above and below the correct line are defined as follows:

$$\Delta y(j) = y(j) - y(j-1),$$

$$\text{for } j = 0, \pm 1, \pm 2, \ldots . \tag{45}$$

Now define a function $\delta y(j)$ which is the y intercept relative to the correct line

$$\delta y(j) = 0, \quad \text{for } j = 0 \tag{46a}$$

$$\delta y(j) = \sum_{g=1}^{j} \Delta y(g), \quad \text{for } j \geqslant 1 \tag{46b}$$

$$\delta y(j) = \sum_{g=1+j}^{0} \Delta y(g), \quad \text{for } j \leqslant -1. \tag{46c}$$

Rewriting (44) so it is centered around the correct line, it becomes

$$P_r = \sum_j P[-k_b \Delta y(j) + \delta y(j) < \hat{\psi}_{12} - (d_{12}/d_{15})\hat{\psi}_{15} + N_{12} - (d_{12}/d_{15})N_{15} < k_b\, \Delta y(1+j) + \delta y(j)] \tag{47}$$

where $j = \ldots -2, -1, 0, 1, 2 \ldots$. See Fig. 12 for a representation of the new orientation.

Assuming the phase measurement errors and the interferometer element spacing errors are Gaussian with zero mean, ε is approximately Gaussian with zero mean. Then (47) becomes

$$P_r = \frac{1}{2} \sum_j \{\mathrm{erf}\{[k_b \Delta y(j+1) + \delta y(j)]/[\sqrt{2}\,\sigma(\varepsilon)]\} - \mathrm{erf}\{[-k_b \Delta y(j) + \delta y(j)]/[\sqrt{2}\,\sigma(\varepsilon)]\}\}. \tag{48}$$

The $\Delta y(j)$ and $\sigma(\varepsilon)$ are in the same units (turns or rads); $\sigma(\varepsilon)$ in turns is given by

$$\sigma(\varepsilon) = [1 + (d_{12}/d_{15})^2]^{1/2}\, [\sigma^2(\psi) + [2\sin^2\theta \sin^2\phi \cdot \sigma^2[d/2)/\lambda^2]]^{1/2}. \tag{49}$$

In (49) it is assumed that $\sigma(\psi_{12}) = \sigma(\psi_{15}) = \sigma(\psi)$, and that $\sigma(d_{12}) = \sigma(d_{15}) = \sqrt{2}\,\sigma(d/2)$. Notice that in (49) $\sigma(\psi)$ is in turns. To determine the number of terms to get a good approximation to (48) let $k_b = \frac{1}{2}$ and add terms until P_r is 1 to within the desired analysis precision.[2]

The probability that the ambiguity is resolved correctly on condition it has been accepted for reduction is determined as was done previously.

$$P_c = \frac{1}{2}\, \{\mathrm{erf}[k_b \Delta y(1)/\sqrt{2}\,\sigma(\varepsilon)] + \mathrm{erf}[k_b \Delta y(0)/\sqrt{2}\,\sigma(\varepsilon)]\}/P_r. \tag{50}$$

It now will be shown, in a heuristic sense, that the optimum condition for resolving the ambiguities is to maximize the distance between lines.

[2]Notice that for the other arm of the interferometer the $\sin^2\phi$ in (49) is replaced by $\cos^2\phi$.

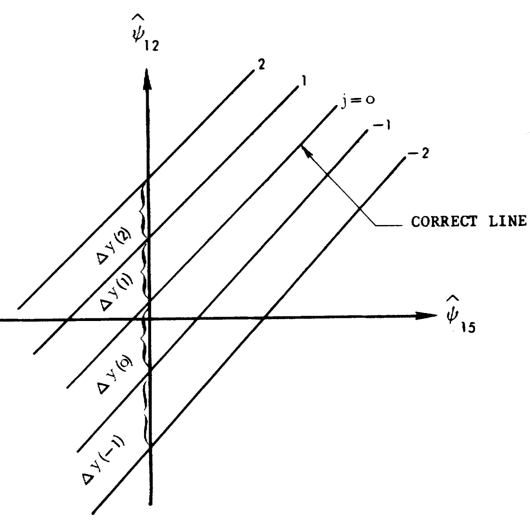

Fig. 12. Sample space labeling about correct line.

In many cases, the optimal ratios of d_{12}/d_{15} result in the $\Delta y(j)$ all being equal, i.e., $\Delta y = \ldots = \Delta y(2) = \Delta y(1) = \Delta y(0) = \Delta y(-1) = \Delta y(-2) = \ldots$. Further, the phase measurement error term frequently dominates in (49) so that $\sigma(\varepsilon) \approx \sigma(\psi)\, [1 + (d_{12}/d_{15})^2]^{1/2}$. Under these assumptions (48) simplifies to

$$P_r = \frac{1}{2} \sum_j \{\mathrm{erf}\{[(k_b + j)\Delta y/\sqrt{2}\,\sigma(\psi)]\, [1 + (d_{12}/d_{15})^2]^{-1/2}\} - \mathrm{erf}\{[(-k_b + j)\Delta y /\sqrt{2}\,\sigma(\psi)]\, [1 + (d_{12}/d_{15})^2]^{-1/2}\}\}$$

$$= \frac{1}{2} \sum_j \mathrm{erf}[(k_b + j)\Delta l/\sqrt{2}\,\sigma(\psi)] - \mathrm{erf}[(-k_b + j)\Delta l/\sqrt{2}\,\sigma(\psi)] \tag{51}$$

where $\sigma(\psi)$ and Δy are on the same units (turns or rads).

The equation $\Delta \ell = \Delta y\, [1 + (d_{12}/d_{15})^2]^{-1/2}$ represents the separation between lines (see (41)). Under the same assumptions,

$$P_c \approx \mathrm{erf}[k_b \Delta l/\sqrt{2}\,\sigma(\psi)]/P_r. \tag{52}$$

If $k_b < \frac{1}{2}$, that is, not all the data is accepted for reduction, the form of P_c is $P_c = A(\Delta l)/[A(\Delta l) + B(\Delta l)]$, where $A(\Delta l)$ represents the term of (51) for $j = 0$ and the numerator of (52) and $B(\Delta l)$ represents all the terms of (51) except the term with $j = 0$.

Differentiating this expression for P_c with respect to Δl we have

$$P_c' = [A'(\Delta l)B(\Delta l) - A(\Delta l)\, B'(\Delta l)]/[A(\Delta l) + B(\Delta l)]^2. \tag{53}$$

By referring to (51) and the definition of $A(\Delta l)$ and $B(\Delta l)$, it can be seen that these two functions are positive for all values of Δl. It can also be shown that $A'(\Delta l)$ is positive for all Δl. If one restricts to the range $\Delta l \geqslant \sigma(\psi)$ it can be shown $B'(\Delta l)$ is negative. Thus, at least for Δl in this range, P_c' is positive and P_c increases as a function of Δl. The restriction $\Delta l \geqslant \sigma(\psi)$ covers the situations of practical interest; for this condition is equivalent to $P_c \geqslant 0.38$ when all the data is accepted. Thus it has been shown that for practical configurations, the system is optimized by maximizing the spacing between lines.

Conclusions

This paper derives several basic equations for an interferometer: expressions for computing the direction of arrival from the phase measurements; expressions for the uncertainty in the direction of arrival based on all system uncertainties; expressions giving the probability that data will be reduced and the probability that ambiguities will be correctly resolved.

Accuracy in the direction of arrival measurement can be increased by increasing the length of the baseline, but this is accompanied by an increase in the possible modulo numbers. As the number of modulo numbers increases, the accuracy with which phase must be measured to maintain the same probability of ambiguity resolution also increases. Therefore, for a given set of uncertainties for phase, frequency, and phase center position, there is a maximum dimension the baseline can have to achieve a given probability of correct ambiguity resolution. This baseline dimension in turn limits direction of arrival accuracy.

These derivations are all based on a limit of three elements to a baseline. By increasing the number of elements, it is possible to increase significantly the direction of arrival accuracy by successively increasing the baseline increment and having each increment resolve the ambiguity for the next larger increment. This was done by Kaufman [5]. No doubt a theory based on an n-dimensional sample space can be developed for an n-element baseline; and this could very well increase insight into this technique.

Some of the important conclusions reached in this article are 1) the baseline does not have to be an integral number of half-wavelengths; 2) there are many optimal positions for the third element in the baseline to resolve ambiguities; 3) a configuration which resolves ambiguities satisfactorily at the highest frequency will do at least as well at any lower frequency. However resolving ambiguities is only part of the problem, and in general, accuracy will decrease with decreasing frequency; 4) restricting the antenna element pattern to the space to be covered by the system will be advantageous to system design; 5) the total number of valid modulo number combinations is less than the number of possible combinations from the individual baselines; 6) maximizing the distance between lines in the sample space is the criterion for optimizing the ambiguity resolution problems; 7) the measurement used to resolve the ambiguity can be utilized to reduce the phase measurement error.

All the error equations are expressed in terms of system parameters and their uncertainties. These uncertainties are a function of many factors, such as signal-to-noise ratios, signal bandwidth, multipath (from ground reflections), atmospheric effects, and polarization. References [2, 8, 9, 11, 12, 13-16] are possible sources for some of this information.

The interferometer can be employed to yield direction-of-arrival accuracy significantly higher than its fundamental accuracy. For example, direction finder fixing [1, 3, 10] when multiple azimuth reception is possible and the Navy space surveillance system [5] both increase the accuracy significantly.

Appendix

The general expressions for the entries in covariance matrix for the basic five element interferometer are as follows:

$$\begin{aligned}\sigma^2(U) = {} & [\lambda\sigma(\psi_{12})\sin\phi/2\pi d_{12}\cos\theta]^2 + [\lambda\sigma(\psi_{34}) \\ & \cdot \cos\phi/2\pi d_{34}\cos\theta]^2 \\ & + [\tan\theta\sin^2\phi/d_{12}]^2[\sigma^2(y_1) + \sigma^2(y_2)] \\ & \quad + [\tan\theta\cos^2\phi/d_{34}]^2[\sigma^2(x_3) + \sigma^2(x_4)] \\ & + [\tan\theta\sigma(f)/f]^2 + [\sin\phi/d_{12}]^2[\sigma^2(z_1) + \sigma^2(z_2)] \\ & \quad + [\cos\phi/d_{34}]^2[\sigma^2(z_3) + \sigma^2(z_4)] \\ & + [\tan\theta\sin2\phi/2d_{12}]^2[\sigma^2(x_1) + \sigma^2(x_2)] \\ & \quad + [\tan\theta\sin2\phi/2d_{34}]^2[\sigma^2(y_3) + \sigma^2(y_4)]. \end{aligned} \tag{54}$$

$$\begin{aligned}\sigma^2(V) = {} & [\lambda\sigma(\psi_{12})\cos\phi/2\pi d_{12}]^2 + [\lambda\sigma(\psi_{34}) \\ & \cdot \sin\phi/2\pi d_{34}]^2 \\ & + [\sin\theta\sin2\phi/2d_{12}]^2[\sigma^2(y_1) + \sigma^2(y_2)] \\ & \quad + [\sin\theta\sin2\phi/2d_{34}]^2[\sigma^2(x_3) + \sigma^2(x_4)] \\ & + [\cos\theta\cos\phi/d_{12}]^2 [\sigma^2(z_1) + \sigma^2(z_2)] \\ & \quad + [\cos\theta\sin\phi/d_{34}]^2[\sigma^2(z_3) + \sigma^2(z_4)] \\ & + [\sin\theta\cos^2\phi/d_{12}]^2[\sigma^2(x_1) + \sigma^2(x_2)] \\ & \quad + [\sin\theta\sin^2\phi/d_{34}]^2[\sigma^2(y_3) + \sigma^2(y_4)]. \end{aligned} \tag{55}$$

$$
\begin{aligned}
\sigma(U, V) = {} & (\sin 2\phi/2 \cos\theta)\{[\lambda\sigma(\psi_{12})/2\pi d_{12}]^2 \\
& - [\lambda\sigma(\psi_{34})/2\pi d_{34}]^2\} \\
& + (\cos\theta \sin 2\phi/2)\{[\sigma^2(z_1) + \sigma^2(z_2)]/d_{12}^2 - [\sigma^2(z_3) \\
& + \sigma^2(z_4)]/d_{34}^2\} \\
& + (\sin^2\theta \sin 2\phi/2\cos\theta)\{(\cos^2\phi/d_{12}^2)[\sigma^2(x_1) + \sigma^2(x_2)] \\
& - (\sin^2\phi/d_{34}^2)[\sigma^2(y_3) + \sigma^2(y_4)] \\
& + (\sin^2\phi/d_{12}^2)[\sigma^2(y_1) + \sigma^2(y_2)] - (\cos^2\phi/d_{34}^2)[\sigma^2(x_3) \\
& + \sigma^2(x_4)]\}. \qquad (56)
\end{aligned}
$$

Acknowledgment

The authors gratefully acknowledge the help and suggestions of L.A. Campbell, S. Evans, Jr., K. Steffan, S.-S. Wang, and H.J. Wertz of the Aerospace Corporation.

References

[1] Stansfield, R.G. (1947)
Statistical theory of D.F. fixing.
Journal of the IEE, (London), 1947, *94* (k) 3A, 762-770.

[2] Simmons, G.J. (1957)
Radio interferometery; errors due to inhomogeneity of medium; theoretical analysis.
IEEE Transactions on Telemetry Remote Control, Vol. TRC-3, Dec. 1957, 2-5.

[3] Ancker, C.J., Jr. (1958)
Airborne direction finding—the theory of navigation errors.
IRE Transactions on Aerospace and Navigational Electronics, Dec. 1958, *ANE 5,* 199-210.

[4] Watters, E.C., Rees, F.L. and Enstrom, R.A. (1961)
High-precision angle determination by means of radar in a search mode.
IRE Transactions on Military Electronics, Oct. 1961, *MIL-5*, 317-325.

[5] Kaufman, M.G. (1964)
Radio interferometer phase-channel combiner Mod. II for the Navy space surveillance system.
IEEE Transactions on Space Electronics and Telemetry, Sept. 1964, *SET-10*, 116-123.

[6] Kendall, W.B. (1965)
Unambiguous accuracy of an interferometer angle-measuring system.
IEEE Transactions on Space Electronics and Telemetry, June 1965, *SET-11*, 62-70.

[7] Margerum, D.L. (1966)
Self-phased arrays.
In R.C. Hansen (Ed.), *Microwave Scanning Antennas, Vol. III: Array Systems,* New York: Academic Press, 1966, ch. 5, 382-390.

[8] Duncan, J.W. (1967)
Microwave interferometers; direction-finders; effects of ground radiation and scattering.
IEEE Transactions on Aerospace and Electronic Systems, Nov. 1967, *AES-3*, 922-932.

[9] Paul, R.H. (1968)
Radio interferometers: refraction error in angle of arrival measurement: analysis.
IEEE Transactions on Aerospace and Electronic Systems, Jan. 1968, *AES-4,* 52-57.

[10] Blachman, N.M. (1969)
Position determination from radio bearings.
IEEE Transactions on Aerospace and Electronic Systems, May 1969, *AES-5*, 558-560.

[11] Titov, A.V. (1969)
Discrete methods of measurement of time position of pulsed signals immersed in noise.
Radio Engineering and Electric Physics, May 1969, *14*, 684-690. (translation of *Radiotechnika i Elektronica*).

[12] Muehldorf, E.J. (1971)
Radio interferometers; multipath distortion of satellite interferometers; angle and position errors.
IEEE Transactions on Aerospace and Electronic Systems, Jan. 1971, *AES-7*, 122-131.

[13] Bennett, J.A. (1971)
Radio interferometers; refractive errors in angle-of-elevation measurements using spaced and single antennas; variational techniques.
IEEE Transactions on Aerospace and Electronics Systems, Mar. 1971, *AES-7*, 243-247.

[14] Muehldorf, E.J., Teichman, M.A., and Kramer, E. (1972)
Polarization mismatch errors in radio phase interferometers.
IEEE Transactions on Aerospace and Electronics Systems, Mar. 1972, *AES-8*, 135-140.

[15] Ipatov, V.P., and Titov, A.V. (1973)
Uniqueness and accuracy of phase measurements in the case of two-frequency radiation.
Radio Engineering and Electronic Physics, Jan. 1973, *18*, 140-144. (translation of *Radiotehnika i Elektronika*).

[16] Titov, A.V. (1974)
Characteristics of two methods of obtaining single-valued phase readings in the case of multifrequency radiation.
Radio Engineering and Electronic Physics, Apr. 1974, *19*, 132-135.

[17] Liebelt, P.B. (1967)
An Introduction to Optimal Estimation,
Reading, MA: Addison-Wesley, 1967, sec. 3-10.

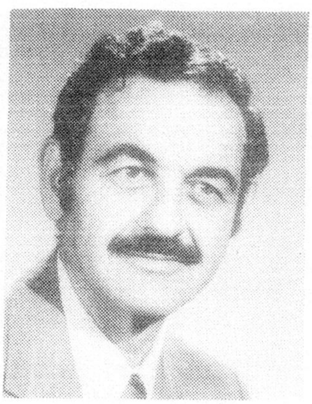

Ernest Jacobs (S'50—A'54—M'59—SM'72) was born in Philadelphia, PA on August 7, 1926. He received the B.S.E.E. and M.S.E.E. degrees from Drexel University, Philadelphia, in 1950 and 1955, respectively, and the Ph.D. degree from the University of Pennsylvania, Philadelphia, in 1961.

His prior employment has been with the Brown Instrument Company, American Electronic Laboratories, Inc., and the University of Pennsylvania. In 1961 he joined the Aerospace Corporation Los Angeles, CA, where he is now a Project Engineer.

Dr. Jacobs is a member of Eta Kappa Nu and Sigma Xi.

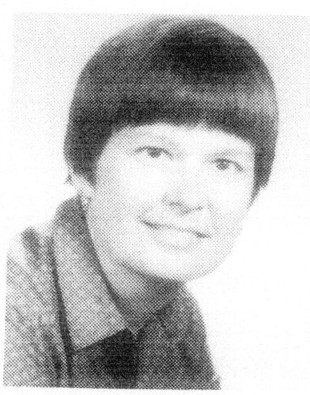

Elizabeth Wall Ralston was born in Urbana, IL, on June 26, 1945. She received the B.S. degree in mathematics from Stanford University, CA, in 1966, and the Ph.D. degree in mathematics from Yale University, New Haven, CT, 1970.

She was on the mathematics faculties of Fordham University (1970-1971 and 1975-1976), California State College, Dominguez Hills, (1971-1973), and the University of California, Los Angeles (1975-1977). Since 1976 she has been with the Aerospace Corporation, El Segundo, CA, where she is currently an Engineering Specialist in the Signal Analysis Software.

Dr. Ralston is a member of the American Mathematical Society and the Association for Women in Mathematics.